EUROPEAN FUSION DEVELOPMENT AGREEMENT

EFDA–JET–PR(03)17

Y. Andrew, N. C Hawkes, M. G. O'Mullane, R. Sartori, M. N. A Beurskens,
I. Coffey, E. Joffrin, D.C. McDonald, R. Prentice, G. Saibene, W. Suttrop,
K-D Zastrow and JET EFDA Contributors

Edge Ion Parameters at the L-H Transition on JET

Edge Ion Parameters at the L-H Transition on JET

Y. Andrew[1], N. C Hawkes[1], M. G. O'Mullane[2], R. Sartori[3], M. N. A Beurskens[1], I. Coffey[4], E. Joffrin[5], D.C. McDonald[1], R. Prentice[1], G. Saibene[3], W. Suttrop[6], K-D Zastrow[1] and JET EFDA Contributors*

[1]Euratom/UKAEA Fusion Association, Culham Science Centre, Abingdon, OX14 3DB, UK
[2]Department of Physics, University of Strathclyde, Glasgow, UK
[3]EFDA Close Support Unit, c/o MPI fur Plasmaphysik, 2 Boltzmannstrasse, 85748 Garching, Germany
[4]Department of Physics, Queen's University, Belfast, UK
[5]Association Euratom/CEA, Cadarache, F13108 St Paul-lez-Durance, France
[6]Max-Plank-Institut fur Plasmaphysik, IPP-Euratom Association, 2 Boltzmannstrasse, 85748 Garching, Germany
**See the appendix of JET EFDA contributors (prepared by J. Paméla and E.R Solano), "Overview of JET Results",*
Fusion Energy 2002 (Proc. 19th Int. Conf. Lyon, 2002), IAEA, Vienna (2002).

Preprint of Paper to be submitted for publication in
Plasma Physics and Controlled Fusion

ABSTRACT.

L-H transition experiments have recently been performed on JET to characterise the local edge ion parameters. Evidence of a threshold in the edge ion temperature to access the H-mode is presented and comparisons are made with edge electron temperature. These results provide the first scaling of pedestal ion temperature on JET. The threshold edge ion temperature scales approximately linearly with toroidal magnetic field and shows no dependence on electron density in the range explored. Reference shots have been repeated with 'reversed field', with the ion ∇B drift away from the X-point and counter neutral beam injection. In contrast to expectations, the reversed field transitions to H-mode occur at very similar values of input power and at lower edge ion and electron temperatures for a range of densities and toroidal fields. The L-H transition is also considered in terms of dimensionless parameter space. The effective edge ion collisionality does not appear to play a significant role in the L-H transition, providing no clear distinction between the L and H-modes phases. In contrast, the normalised poloidal ion gyroradius provides a sharp H-mode boundary at any given field and current, consistent with a threshold ion temperature for H-mode access being dependent on toroidal field but not on density. However, comparison of ρ^* and ν_i^* with forward and reversed fields, across a range of fields and currents demonstrates that these dimensionless parameters simply describe an operation trajectory for the JET L-H transition.

1. INTRODUCTION

The H-mode is an edge phenomenon characterised by the formation of a steep edge transport barrier, typically a few centimetres wide on JET [1], and by an increase in particle and energy confinement times. Since, the H-mode is the reference operation regime for the next step device, ITER [2], there has been considerable effort over the past few years to measure the edge plasma parameters over a wide range of conditions. Experimental evidence has been presented from several machines to indicate that a critical edge electron temperature, T_e, is necessary for the transition to H-mode [3, 4, 5, 6, 7]. Further studies suggest that a closely related threshold parameter such as the edge ion temperature, T_i, the ion temperature gradient, ∇T_e or ion gyroradius may be the necessary condition for accessing and maintaining the H-mode[6, 7, 8, 9]. However, there has been relatively much less documentation of the pedestal T_i at the transition to H-mode and it has often been assumed to be equal to the edge T_e in L-H transition studies on JET [7, 10].

The dependence of the edge T_i on density and its relation to the L-H transition power threshold has been extensively explored on JT-60U [8]. The edge T_i measured at $\psi = 0.95$, was found to be the most influential element in the increased input power required for the transition to H-mode at very low edge electron densities, $n_e < 1.2\times10^{19}$ m^{-3}. In the range $n_e < 1.2\times10^{19}$ m^{-3}, the effective edge ion collisionality, $\nu_{i,\,eff}^{95}$ decreased significantly with reduced density corresponding to increased L-H transition threshold power. The lower values of $\nu_{i,\,eff}^{95}$ was found to be directly linked to higher edge T_i at increased threshold power. Similar studies carried out on JET showed the L-H transition power threshold to increase for values of edge $n_e < 1.2\times10^{19}$ m^{-3} at $B_t = 2.6$T with an associated

increase in edge T_e [7, 11]. The dependence of the edge Ti on toroidal field, Bt, has been studied on DIII-D [12] fo the range of 1-2T in both forward and reversed field directions. The edge Ti at the L-H transition was reported to increase almost linearly with Bt for either sign of the field and to be two times larger with reverse Bt than in the forward direction. Previous measurements of the edge on temperature on JET using active charge exchange spectroscopy at the L-H transition has been presented in [1, 13, 14, 15]. The main results were that the edge Ti barrier width increases (3-4cm) with increasing Ti while maintaining a constant maximum gradient and awidth similar to the H-mode edge Te barrier [1]. In [14] it was reported that the effective edge ion collisionality, vieff does not appear to play a significant role in the transition to H-mode on JET, while Ti-3/ Zeff remained constant at the start and end of the ELM-free phase of the density scan examined

The main aims of this paper are to present results from the first dedicated experiments to systematically examine the dependence of the JET pedestal ion parameters at the L-H transition on both n_e, B_t, ion ∇B drift direction and to compare the pedestal T_i with T_e values. The n_e and B_t scan experiments along with the diagnostics that have been used are described in section 2. The experimental results are presented and discussed in the following section. The parameters considered include the edge, T_i, T_e, the impurity corrected edge ion collisionality,and the normalised poloidal ion gyroradius, ν_i^* and the normalised poloidal ion gyroradius ρ^*. Finally a brief summary of the results and the conclusions from the study are given in section 4.

2. EXPERIMENT

The edge T_i profile is measured on JET using C^{6+} impurity charge exchange recombination spectroscopy (CXRS) with neutral beam heating (NBI). The interpretation of the CXRS T_i measurement assumes the impurity ion temperature to be the same as the main plasma T_i. The edge CXRS diagnostic on JET also measures the C^{6+} ion density profiles, n_z, necessary for calculating the effective edge ion collisionality. A detailed description of the original experimental set-up of the JET edge CXRS diagnostic is given by Hawkes et al. in [13] and is not described in any further detail in this paper.

The L-H transition is characterised by either a sharp drop in the D_α signal or by its change to a dithering phase as shown in the example in figure 1, and both these phases are followed by an ELM-free period. It is interesting to note that L-H transitions into an ELM-free phase only occurred in plasmas with B_t =2.1T, which represented less than 25% of all the shots included for this paper. All other plasmas with higher values of B_t had transitions to a dithering or type III ELMy H-mode phase, with ion ∇B drift both towards and away from the X-point.

The edge CXRS system has a time resolution of 50 ms which of necessity defines the time slices used in the evaluation of the edge T_i. Several time slices have been considered in the analysis and include an L-mode point taken 0.5s before the transition, the two CXRS time points on either side of the L-H transition, the last CXRS point before the transition to the ELM-free phase and the CXRS time point preceding the first type I ELM. The pedestal ion temperature, T_i^{ped} at the transition to H-mode has been calculated by measuring the ion temperature prior to and following the L-H

transition, as shown by the vertical dotted lines in figure 1. T_i^{ped} has been interpolated to the time of the L-H transition defined by the drop in the D_α signal or its change to the dithering phase. By considering several time slices from the L-mode through to the first ELM, a detailed picture is obtained of how the edge T_i^{ped} evolves across the transition to H-mode. This approach provides a clearer comparison of parameters between different discharges, than using a single L-H transition time slice. For most of the shots included in this study the transition back to L-mode occurs after the NBI heating has been switched off and very little CXRS data is available for the H-L transition phase.

Since the pedestal is the region of interest for L-H transition studies [4, 12], the edge ion and electron temperatures presented in this paper have been measured at the top of their respective pedestals. Typical edge ion and electron temperature profiles for this study are shown in figure 2 along with the location of the top of the ion and electron temperature pedestals. For both the T_i and T_e profiles the top of the pedestal is identified by the discontinuity in the gradient as defined in previous JET studies [1, 10]. The T_e profiles have been measured using a multichannel ECE radiometer with a time resolution of 1ms.

The line integrated, edge electron density is measured with an interferometer along a single chord at a mid-plane radius of $R_{mid} = 3.74$ m for these shots. The edge line average density has been calculated by dividing the measured line integrated density by the chord length in the plasma.

All the plasmas studied had lower single null magnetic configurations with both inner and outer strike points on the vertical targets of the JET Mark II Gas Box Septum Replacement Plate (MkII GB SRP) divertor [16]. NBI is the only additional heating method in the shots considered and they have slow power ramps at rates of between 1-3MW/s, as shown in the example in figure 1. These plasmas were fuelled with deuterium and had hydrogen concentrations of less than 1%. For the density scan experiment at 2.0MA/2.4T the edge line averaged density of the plasmas was varied from 1.3×10^{19} m^{-3} to 2.0×10^{19} m^{-3} at the L-H transition. The lower limit of the scan is defined by the minimum density of operation with NBI required for the CXRS measurement of edge T_i, while the upper range is set by the L-mode density limit. The reference shots (forward B_t) were repeated for a range of values with the ion ∇B drift away from the X-point and counter neutral beam injection to study the effect on the L-H transition power threshold and edge temperatures. These shots are referred to as having reversed B_t in this paper.

3. H-MODE THRESHOLD

3.1. DENSITY DEPENDENCE

The rate of change of stored plasma energy, $\dot{W}_{dia}$, has been subtracted from the total input power for each of the L-mode, L-H transition, ELM-free and first ELM time slices described in section 2 and these values of corrected power are shown as a function of the edge line averaged electron density, n_e, in figure 3. The corresponding $T_i^{ped}$and T_e^{ped} values are also plotted as a function of n_e in figure 4. While the L-H transition power threshold increases from 5.5-8.8MW with increasing edge density, the edge T_i and T_e values at the transition to H-mode show very little variation, as

shown in figure 4. As the discharges progress into the ELM-free and type I ELM phases of the H-mode both the edge T_i and T_e show much more scatter, and the pedestal temperatures provide a clear separation between the L-mode and H-mode phases. These results are interpreted as a strong indication that a threshold T_i, T_e or related parameter, rather than a power flux threshold, is required to access the H-mode on JET. The edge density range considered here is similar to the higher density ranges explored in the JT-60U n_e scan in [8, 17, 18] and eliminates the influence of increased threshold power observed for $n_e < 1.2\times10^{19}$ m^{-3}. However, the JET results differ from observations on JT-60U that the edge ion temperature, T_i^{95} increases with edge density above 1.2×10^{19} m^{-3} [8].

Figure 4 also shows that $T_i^{ped} = 2T_e^{ped}$ at the L-H transition and that T_i^{ped} remains higher than T_e^{ped} through to the end of the higher density ELM-free phase at $n_e = 3\times10^{19}$ m^{-3}. Comparison of the T_i and T_e profiles in figure 2 show that the location of the tops of the pedestals are found to be very close, agreeing to within 2cm.

3.2. B_t DEPENDENCE

The B_t scaling of the threshold T_i^{ped} has been examined by considering all NBI induced L-H transition experiments with slow power ramp rates of typically 1-3 MW/s, for which edge CXRS measurements were available. The measured L-H transition threshold power for these shots are plotted in figure 5 as a function of the threshold power scaling from Snipes et al. [19], $P_{th} = 0.05B_t n_e S$, where n_e is the central line average density (in units of 10^{20} m^{-3}) and S is the plasma surface area (in m^2). The dependence of T_i^{ped} and T_e^{ped} on B_t, is shown in figure 6 and for this set of discharges the edge n_e varies from 1.0×10^{19} m^{-3} to 2.2×10^{19} m^{-3} and B_t is varied from 1.0 - 3.45 T. The plasma triangularity, δ is constant at around 0.22 and q_{95} varies from 3.1-3.9. These results further show T_e^{ped} to be lower than T_i^{ped} at the L-H transition for the n_e range included within this B_t scan. The variation of T_i with B_t on JET is similar to that reported from DIII-D [12]. The B_t range explored on JET has been extended beyond that presented in [12] and an unconstrained fit to the forward B_t data shown in figure 6 gives the dependence:

$$T_i^{ped} = 497 n_e^{0.06(\pm0.12)} B_t^{0.83(\pm0.09)} \text{ eV} \quad (1)$$

Comparison of the reversed B_t discharges with reference forward field plasmas in figures 5 and 3, shows the L-H transition power threshold to be very similar for both the density and B_t scans. At the lowest toroidal field of 1.2 T, the transitions to H-mode were very clearly defined by a sharp drop in the divertor D_α signal, straight into an ELM-free phase. With increasing reversed field and plasma current, the transition became less obvious to identify, with gradual evolution of the plasma parameters to dithering or a Type-III ELMy H-modes. However, all the reversed field L-H transitions included in this study can be identified to within 200ms and since the power ramps were slow, 1MW/s, the level of uncertainty in the threshold power and local edge parameters is around 5%. Despite having very similar power thresholds to the forward field shots, the reversed field T_i^{ped} and T_e^{ped} values at the

L-H transition are lower, as shown in figure 6, although the approximate linear dependence on B_t is similar. These results are in contrast to the much high power thresholds and edge temperatures required on DIII-D [12, 20] and ASDEX-U [4] at the transition to H-mode with reversed field. However, this difference may in part be explained by definitions used for the start of the H-mode. On JET the reversed field power thresholds for ELM-free and type-I ELM phase access, following a long dithering phase at 2.4T, are also up to twice those with forward field for similar edge densities as shown in figure 3.

3.3. DIMENSIONLESS PARAMETERS

The local edge ion data from the density and B_t scans described in the previous two sections is plotted in terms of dimensionless operation space in figure 7 using the normalised poloidal ion gyroradius $\rho^* = \rho_{i,p}/R$, and the effective normalised ion collisionality, ν_i^*. The effective edge ν_i^* has been calculated using the modified expression from Hawkes et al. [14] which accounts for ion-impurity and impurity-impurity collisions:

$$\nu_i^* = \frac{\nu_{ii} R q}{v_t \epsilon^{3/2}} \left\{ 1 + 2\sqrt{2}\frac{n_z}{n_i} Z^2 + \left(\frac{n_z}{n_i}\right)^2 Z^4 \sqrt{\frac{m_z}{m_i}} \right\}, \tag{2}$$

where, n_z is the carbon density measured with the edge CXRS, n_i is the main plasma ion density taken to be $(n_e - n_z Z)$, and m_z and m_i are the carbon and deuterium ion mass respectively. The electron density and therefore the carbon ion density, are both measured at $R_{mid} = 3.72$m, which corresponds to the measured first point within the top of the T_i pedestal. Hence, ν_i^* is also calculated for this radial location. The values of edge ν_i^* at the L-H transition range from 1.0 to 1.9 despite the constant T_i across the density scan considered in figure 7. Therefore, the impurity ion density, n_z tends to compensate for reducing n_i in the density scan resulting in a relatively narrow range of effective collisionality at the transition to H-mode. However, there is a great deal of overlap between the L-mode and H-mode ν_i^* values. In contrast, ρ^* values show little variation at $\rho^* = 0.005$ across the density scan in figure 7 at the H-mode transition and provide a very clear boundary between L and H-mode phases. This result is consistent with that reported from ASDEX Upgrade [4] where the experimental variation in the vicinity of the H-mode was found to be very small at around $\rho^* = 0.001$.

Consideration of all the shots within the B_t scan maps out the JET operation trajectory in figure 8 for the L-H transition as a function of ρ^* and ν^*. The solid line represents the expected dependence of ρ^* on ν^* using equation 1, at a fixed density of 2.5×10^{19}m^{-3}. The width of the operation envelope is determined by the range of n_e values accessible at the L-H transition on JET. These results show that ν_i^* spans a wide range of values, ranging from 0.6-3.9 at the transition to H-mode on JET, in contrast to theories in which a critical ν_i^* is the determinant for H-mode access [21, 22]. The reversed B_t shots have a lower ρ^* L-H transition boundary than those with forward B_t, reflecting the lower threshold T_i^{ped} values for achieving H-mode. Examination of the full dataset in figure 8 therefore indicates that the dimensionless parameters and cannot be used to predict the transition to H-mode.

CONCLUSIONS

Previous studies of the edge ion parameters on JET have concentrated on the H-mode [1, 13, 14, 15]. That work has now been extended in this paper to fully characterise the L-H transition itself across a wide range of experimental conditions. The edge plasma density has been scanned with fixed B_t and I_P, resulting in an increase in the L-H transition power threshold with increasing density. The T_i^{ped} is found to reach a fixed value at the L-H transition, showing no significant density dependence. The T_i^{ped} shows similar behaviour at the transition to H-mode, also providing a clear distinction between the L and H-mode states. These results imply that a criterion for the L-H transition is that the edge T_i, T_e or some function of these parameters, reaches a threshold value. T_e^{ped} is a factor of two lower than T_e^{ped} at the transition to H-mode and a difference between the two temperatures is maintained as all the discharges considered evolve through to the higher densities of the first ELM.

By considering all the recent dedicated JET L-H transition experiments with CXRS data, T_i^{ped} is found to scale as $B_t^{0.83}$ and is higher than T_e^{ped} across the full range of B_t = 1-3.45T. The power threshold for the L-H transition has been measured to be very similar for both the forward and reversed field directions on JET, while both T_i^{ped} and T_e^{ped} are found to be lower with the reversed field.

The local edge dimensionless ion parameters, ρ^* and ν_i^*, have been examined for the density and B_t scan experiments performed. The edge ion collisionality, ν_i^*, is calculated to range from 0.6-3.9 at the L-H transition and does not provide a clear distinction between L and H-mode phases. In contrast, due to the lack of density dependence of T_i^{ped}, ρ^* provides a very sharp separation between L and H-mode phases at any given field and current. However, inspection of the full dataset shows that while the ρ^*, ν_i^* space maps out the L-H transition operational trajectory on JET, it does not provide a threshold boundary for H-mode access.

ACKNOWLEDGEMENTS

This work has been performed under the European Fusion Development Agreement (EFDA) and was funded partly by the United Kingdom Engineering and Physical Sciences Research Council and by Euratom.

REFERENCES

[1]. Breger P et al., Plasma Phys. Control. Fusion **40** (1998) 347-359.

[2]. Pacher GW et al., Nucl. Fusion **43** (2003) 188-195.

[3]. Snipes JA et al, Plasma Phys. Control. Fusion **38** (1996) 1127-1136.

[4]. Suttrop W et al., Plasma Phys. Control. Fusion **39** (1997) 2051-2066.

[5]. Y Takase Phys. Plasmas **4** (1997) 1647.

[6]. Hubbard AE, Boivin RL, Drake JF, Greenwald M, In Y, Irby JH, Rogers BN, and Snipes JA, Plasma Phys. Control. Fusion **40** (1998) 689-692.

[7]. Righi E, Campbell DJ, Conway GD, Hawkes NC, Horton LD, Maggi CF, Saibene G, Sartori

R and Zastrow K-D, Plasma Phys. Contol. Fusion **42** (2000) A199-A204.
[8]. Fukuda T, Takizuka T, Tsuchiya K, Kamada Y, Nagashima K, Sato M, Takenaga H, Ishida S, Konoshima S, Higashijma S, Tobita K, Kikuchi M, Mori M Nucl. Fusion **37** (1997) 1199-1213.
[9]. Groebner RJ et al., Physics of Plasmas **8** (2001) 2722.
[10]. Righi E et al., Nucl. Fusion, **39** 3 (1999) 309-319.
[11]. Horton LD, et al, 1999, 26th EPS Conf. on Controlled Fusion and Plasma Physics (Maastricht).
[12]. Groebner RJ and Carlstrom TN, Plasma Phys. Control. Fusion **40** (1998) 673-677.
[13]. Hawkes NC and Peacock N, Rev. Sci. Instrum. **63**(10) (1992) 5164
[14]. Hawkes NC, Thomas P,Control. Fusion and Plasma Phys., 20th EPS Conf. Lisbon,(1993) I-7-I-10.
[15]. Hawkes NC, Bartlett DV, Campbell DJ, Deliyanakis N, Giannella RM, Lomas PJ, Peacock NJ, Porte L, Rookes A and Thomas PR, Plasma Phys. Control. Fusion **38** (1996) 1261-1266.
[16]. Pamela J, Rapp J, 'Overview of JET results, near term plans', 22nd SOFT Conf. Helsinki, (2002).
[17]. Fukuda T, Plasma Phys. Control. Fusion **40** (1998) 543-555.
[18]. Fukuda T et al., Plasma Phys. Control. Fusion **40** (1998) 827-830.
[19]. Snipes JA et al., for the ITPA Confinement and H-mode Threshold Database Working Group, (Proc. 19th IAEA Fusion Energy Conf., Lyon, 2002), paper IAEA-ITERCT-P/04.
[20]. Carlstrom TN, Burrell KH, Groebner RJ, Plasma Phys. Control. Fusion **40** (1998) 669-672.
[21]. Shiang KC, Crume EC, and Houlberg WA, Phys. Fluids B, 2 6 (1990) 1492.
[22]. Shiang KC, Hsu CT, Zhang YZ, Plasma Phys. Control. Fusion **38** (1996) 1331-1335.

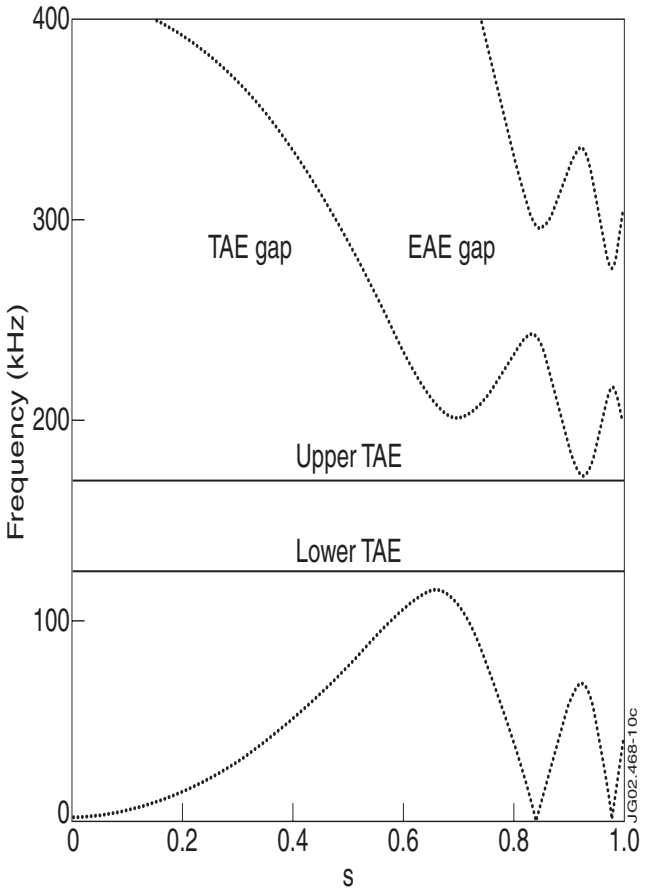

Figure 1: Inner divertor D_α signal and mid-plane T_i and T_e values at the pedestal top for Pulse No: 56611 from the density scan experiment at 2.0MA/2.4T. The dashed, vertical lines on the D_α trace correspond to the T_i measurement timing, across the L-H transition. The smoothed total input power, the stored magnetic energy and the edge line average n_e are also shown.

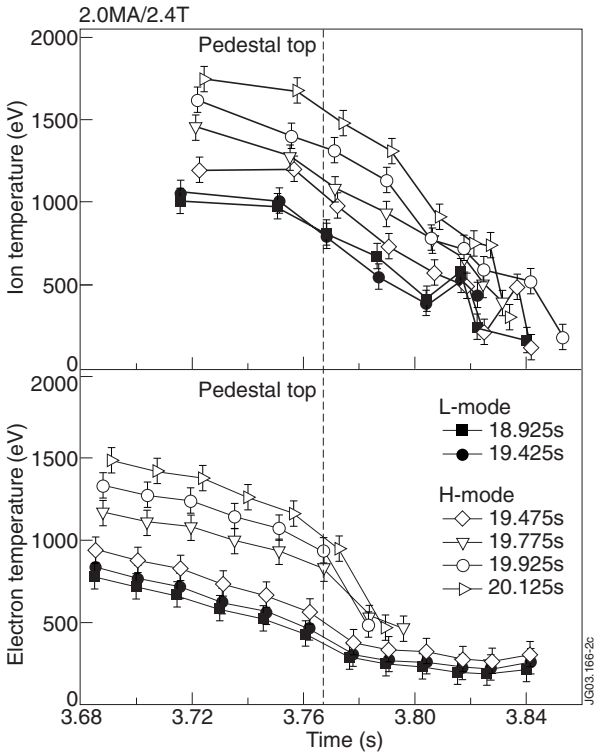

Figure 2: Example of the evolution of the edgeT_i and T_e profiles from L-mode through to the end of the ELM-free phase for Pulse No: 56611. The top of the pedestal is indicated for both T_i and T_e by dashed vertical lines.

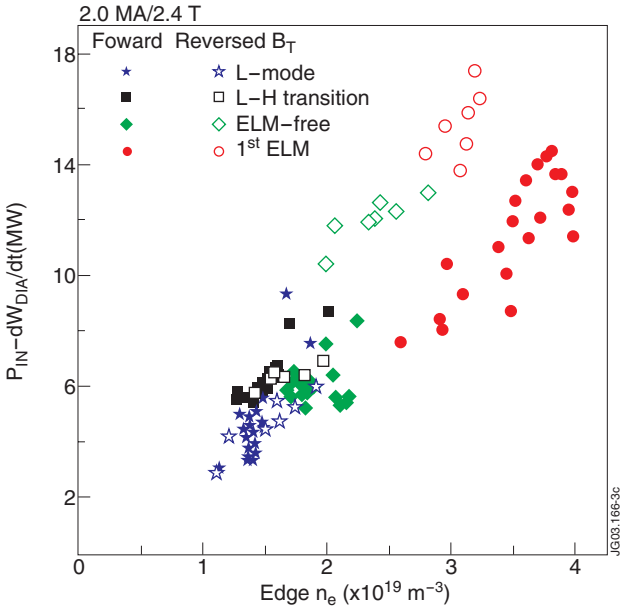

Figure 3: Input power plotted as a function of line average edge electron density at 2.0MA/2.4T for forward and reversed field.

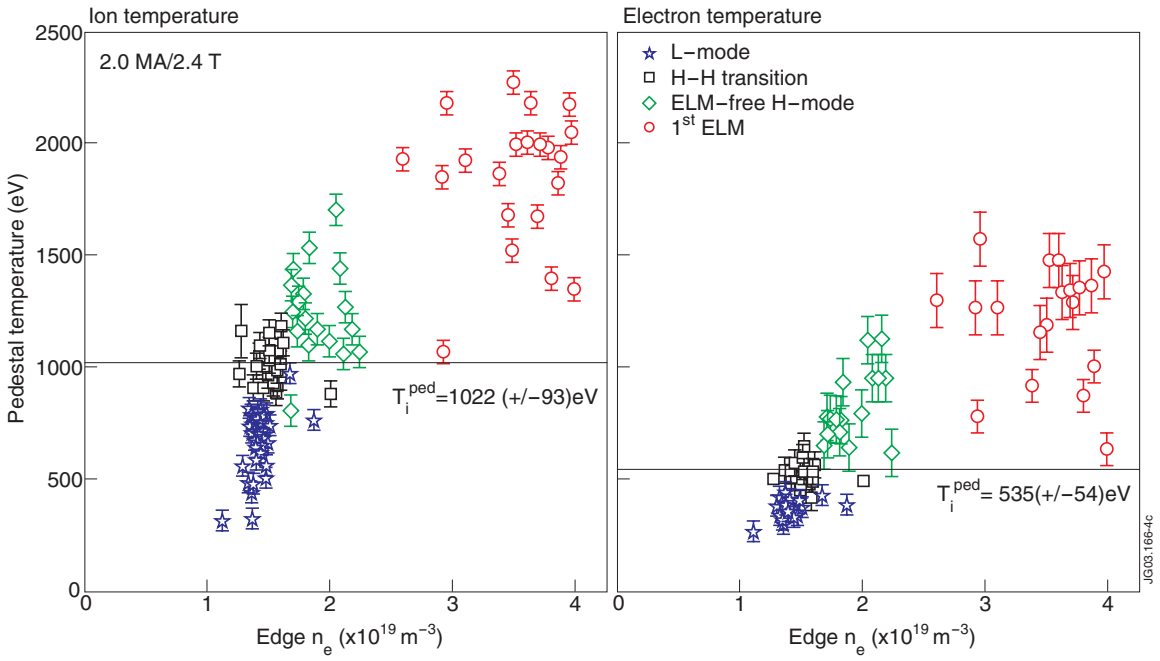

Figure 4: T_i^{ped} and T_e^{ped} values electron density at 2.0MA/2.4T with ion ∇B drift direction towards the X-point.

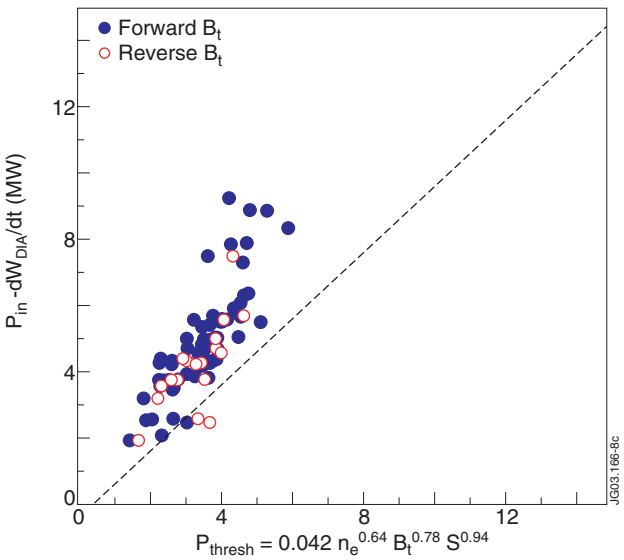

Figure 5: SMeasured threshold power for both forward and reversed field plotted as a function of the threshold power scaling taken from [19].

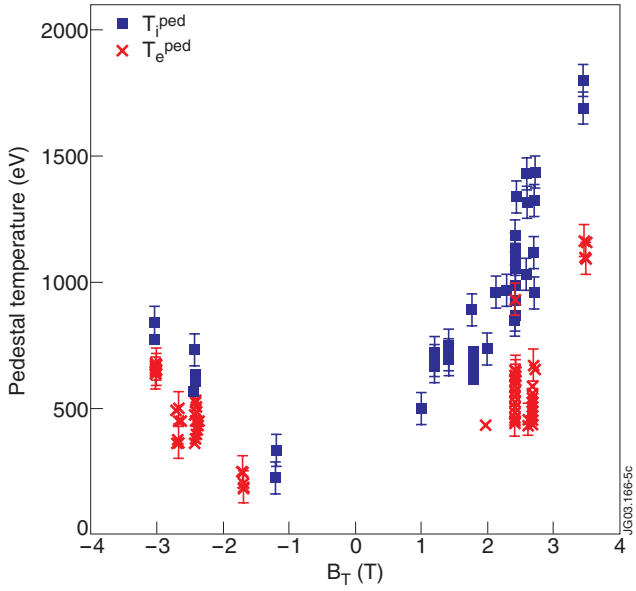

Figure 6: Scaling of T_i^{ped} and T_e^{ped} at the L-H transition with toroidal magnetic field, B_t, in both forward and reverse directions. the positive values of Bt correspond to ion ∇B towards the X-point, while negative Bt have ion ∇B directed away

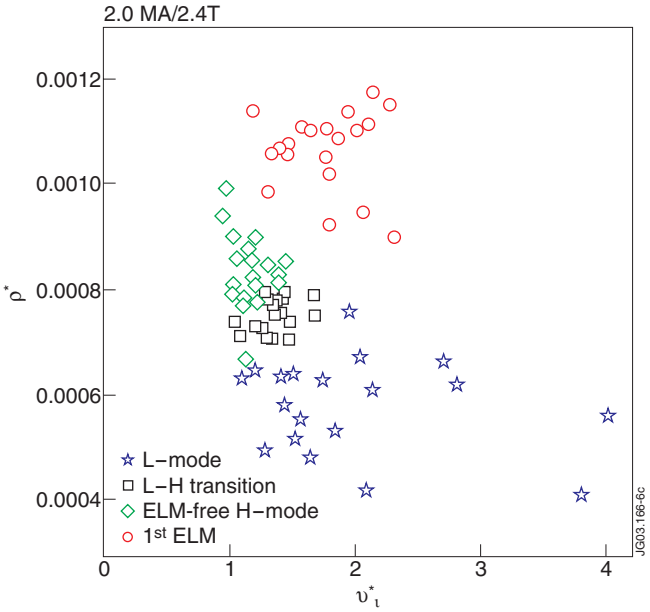

Figure 7: L-mode and H-mode phases in normalised poloidal ion gyroradius, ρ, and effective normalised collisionality, ν_i*, operation space.*

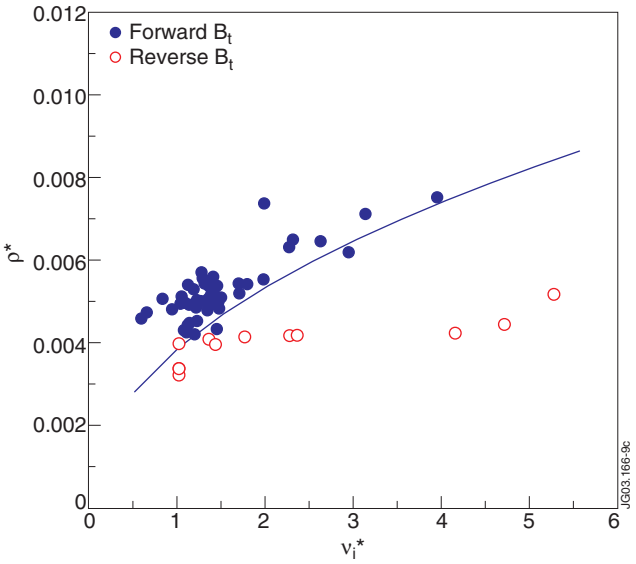

Figure 8: Normalised poloidal ion gyroradius,ρ, versus effective normalised collisionality, ν_i*, at the L-H transition for all forward and reversed B_t discharges considered in section 3.2. The solid line represents the expected dependence of ρ* and ν* using equation 1 (see text)*